ADVANCED MATERIALS

DOI: 10.1002/adma.200601551

Self-Lubricating Nano-Ball-Bearings**

By *Chad M. Brick*, *Elaine R. Chan*, *Sharon C. Glotzer*, *Julien C. Marchal*, *David C. Martin*, and *Richard M. Laine**

Cubic symmetry in octasilsesquioxanes ($[RSiO_{1.5}]_8$, diameter 1 nm) places functionality in each octant in Cartesian space, enabling nanometer-scale construction of materials with subtle tailoring of global properties.[1–3] Diverse studies of OPS (octasilsesquioxanes) range from their ordering in solids (nanocomposites) to catalysts, NMR standards, and spacecraft coatings.[4–13] The prototypical OPS[10] (R = phenyl) is air-stable to temperatures above 500 °C; however, high symmetry and crystallinity limit its maximum solubility to 100 mg per 100 mL CH_2Cl_2, rendering attempts at functionalization very difficult.[10,12,13]

In an effort to couple early work on liquid-crystalline (LC) silsesquioxanes with recent efforts to functionalize OPS, we explored Friedel–Crafts alkylation[14] by $AlCl_3$, despite the potential for Si–C bond cleavage.[15] However, its easy nitration in fuming HNO_3 offered encouragement.[10] The impetus was to add sufficient alkyl groups to disrupt registry between OPS molecules, thereby reducing crystallinity to produce LC and/or high-temperature lubricants.[16]

Here, we report that Friedel–Crafts alkylation of OPS leads to alkyl$_x$OPS materials with rigid 1 nm cores, which are surrounded by a hydrocarbon layer that acts as a lubricant to these hard spheres or nano-ball-bearings. Surprisingly, the butyl and hexyl derivatives are air-stable and liquid over a 70–400 °C range, whereas the octyl and decyl derivatives are stable only over a 30–300 °C range. Molecular modeling studies suggest that the unusual 100 °C difference in thermal stability arises because the shorter chains interdigitate even in the liquid state. This behavior is similar to that predicted and seen recently for alkylthiol-modified superlattices,[17,18] suggesting that alkyl$_x$OPS materials may serve as models of superlattices. These materials offer potential as high-temperature lubricants. Furthermore, interdigitation suggests that alkyl$_x$OPS-based systems might serve as nanogears or as nanoscale Velcro when affixed to surfaces.

Friedel–Crafts alkylation (nRBr, see Supporting Information) of OPS produces alkyl$_x$OPS, with typical[14] 7:3 ratios of branched/normal alkyl groups. Cleavage of Si–C bonds (by using nBu_4NF) coupled with analysis by ^{13}C NMR and matrix-assisted laser desorption ionization time-of-flight mass spectrometry (MALDI-TOF MS, see Fig. S1 in the Supporting Information) distinguish individual alkylation products and the average numbers of alkyl groups per phenyl for each nRBr. Table 1 summarizes the results of gel-permeation chromatography (GPC) and viscosity measurements. Table 2

Table 1. Analytical data for OPS alkylated at various reaction times. M_w: weight-average molecular weight, M_n: number-average molecular weight, PDI: polydispersity index. 1 Da = 1.66×10^{-27} kg.

R	Time [h]	M_w [Da]	M_n [Da]	PDI	Viscosity [a] at 80 °C [10^3 mPa s]
Butyl	1	852	913	1.07	
	5	1035	1058	1.02	
	10	1116	1196	1.07	68
	24	1215	1288	1.06	
Hexyl	1	1021	1102	1.08	
	5	1184	1204	1.02	
	10	1298	1394	1.07	25
	24	1416	1574	1.11	
Octyl	1	950	1002	1.05	
	5	1063	1120	1.05	
	10	1253	1302	1.04	6
	24	1592	1775	1.11	
Decyl	1	911	952	1.05	
	5	1414	1516	1.07	
	10	1649	1738	1.05	2
	24	2160	2459	1.14	

[a] Viscosities were measured by using a parallel plate Rheometric RDS II E. Shear rate 10 s^{-1}, gap 1 mm.

[*] Prof. R. M. Laine, Prof. S. C. Glotzer, J. C. Marchal, Prof. D. C. Martin
Department of Materials Science and Engineering
University of Michigan
Ann Arbor, MI 48109-2136 (USA)
E-mail: talsdad@umich.edu
Prof. R. M. Laine, Prof. D. C. Martin
The Macromolecular Science and Engineering Center
University of Michigan
Ann Arbor, MI 48109-2136 (USA)
Dr. C. M. Brick
Dow Corning Corporation
Corporate Center
PO Box 994
Midland, MI 48686-0994 (USA)
E. R. Chan, Prof. S. C. Glotzer
Department of Chemical Engineering
University of Michigan
Ann Arbor, MI 48109-2136 (USA)

[**] ERC and SCG thank the National Science Foundation (NSF) for financial support under grant DMR-0103399. DCM also acknowledges partial support from the NSF. RML and CMB thank the NSF for an IGERT grant for partial support of this work, AFRL at Edwards AFB and Guardian Industries for partial support. We would especially like to thank C. James and J. Chen for reproducing key results and for video images of the mechanical deformation associated with the melting processes. We also thank Dr. R. Vaia for pointing out the superlattice modeling and melting studies. Supporting Information is available online from Wiley InterScience or from the author.

Table 2. X-ray diffraction data (XRD) for OPS alkylated at various reaction times [a].

R	5 h		10 h		24 h	
	2θ	d [Å]	2θ	d [Å]	2θ	d [Å]
Butyl	7.3°	12.1	6.9°	12.8	6.6°	13.4
	18.6°	4.8	17.8°	5.0	18.4°	4.8
	21.6°	4.1	21.5°	4.1	20.6°	4.3
	26.8°	3.3	26.5°	3.4	26.5°	3.4
					40.6°	2.2
Hexyl	7.4°	11.9	6.6°	13.4	6.2°	14.2
	18.1°	4.9	–	–	16.6°	5.3
	20.2°	4.4	20.2°	4.4	20.8°	4.3
	24.2°	3.7	26.3°	3.4	25.3°	3.5
Octyl [b]			7.9°	11.2		
			18.7°	4.7		
			23°	3.8		
			39.7°	2.3		
Decyl [c]	6.6°	13.4	5.9°	15.0		
	19.8°	4.5	18.2°	4.9		
	–	–	20.2°	4.4		
	23.4°	3.8	24.3°	3.7		

[a] No XRD patterns were obtained for 1 h reaction times for all alkyl groups. [b] No XRD patterns were obtained for 5 and 24 h reaction times. [c] No XRD pattern was obtained for a 24 h reaction time.

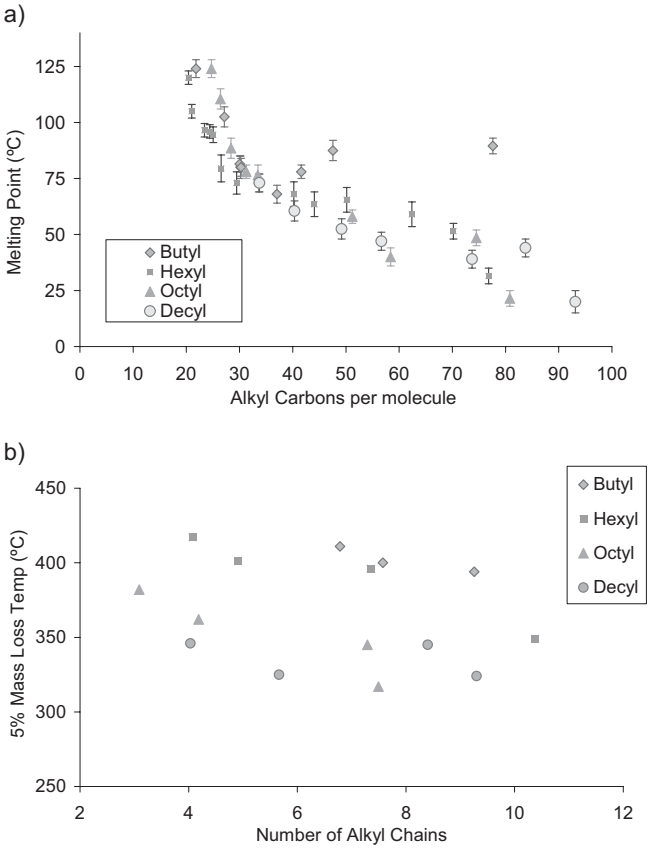

Figure 1. a) Melting points of alkyl$_x$OPS materials. Each point averages two or more runs, and is the midpoint in the melting process. b) Thermal stabilities of alkyl$_x$OPS, heated at 10 °C min^{-1} to 5 % mass-loss temperature.

shows powder X-ray diffraction (XRD) data for selected products (see also Figs. S2–S6). Figure 1a plots the melting points (T_ms) of these materials versus the number of alkyl carbons per molecule, whereas Figure 1b plots the thermal stabilities of these compounds on heating in air at 10 °C min^{-1} to their 5 % mass-loss temperature ($T_{d5\%}$).

Efforts to identify LC phases by differential scanning calorimetry (DSC) failed, as only small, broad features occurred that could not be related to any phase transitions. However, the 24 h butyl and hexyl products showed endotherms centered at 70 °C (< 10 °C full-width at half maximum), associated with T_ms. Optical microscopy (OM) of samples heated under crossed polars showed no birefringence that could be associated with LC behavior.

Hot-stage OM indicates that the transition temperatures associated with the DSC endotherms correlate with the onset of flow behavior, indicating true melting transitions. At low temperatures, the samples are solids and deform plastically on scratching. At high temperatures, they flow into uniform, liquid thin films (a video is available in the Supporting Information). Both the solid and liquid phases are isotropic, with limited evidence for birefringence.

Given the extensive branching, it is surprising that XRD patterns of samples that were melted, cooled, and ground showed significant ordering (Table 2). The peaks at the lowest angles had full-width at half height 2θ values of 6°–7°. Those at higher angles were much broader. Based on the work of Waddon and Coughlin,[14a] we can use curve fitting and hexagonal packing to perform best-fit deconvolution of these XRD patterns. From the data in Table 2, and the XRD patterns in Figures S2–S6, we see that the extent of alkylation is clearly indicated by the increase in d-spacing as a function of reaction time (degree of alkylation) for both the butyl and hexyl derivatives. The decyl XRD patterns are similar, but significant changes in peak intensities suggest poorer ordering (only limited data was taken for the octyl materials). However, the first decyl peaks are at the shortest 2θ values, associated with the greatest separation between the cores of ca. 15 Å at 10 h reaction time.

Perhaps the most interesting observations are the ca. 100 °C differences in thermal stabilities for the butyl$_x$OPS and hexyl$_x$OPS versus octyl$_x$OPS and decyl$_x$OPS, and the clear upturn in T_m for the butyl$_x$OPS. Bolln et al. recently synthesized the simple linear octaalkylsilsesquioxanes from ethyl to decyl.[19] These materials showed thermal stabilities in air similar to the octyl and decyl systems studied here. Decomposition onsets are all ≤ 300 °C, with complete decomposition occurring near 400 °C. This type of thermal stability is common for simple alkyls, and consequently our observation of oxidative stabilities above 400 °C is quite unique.

Although only limited viscosity studies are presented here, they seem to correspond with the separation distances between the cores, suggesting that higher degrees of alkylation will lead to lower viscosities within a series. This will be verified in more complete studies at a later time.

ADVANCED MATERIALS

On a statistical basis, a unique feature of the butyl and hexyl compounds is that they have a higher tertiary/benzyl hydrogen content than the octyl and decyl materials, because of extensive branching. Therefore, they should, in principle, be highly susceptible to oxidation; however, they are the most stable.

Bolln et al. also observed that the T_ms of the longer-chain compounds exhibited odd–even effects, where the even-chain materials melted at temperatures that were 5–10 °C higher than adjacent odd-chain compounds. The lowest observed T_m, at ca. 25 °C, was obtained for the n-pentyl compound. Longer chain lengths exhibited an upturn in T_m to ca. 60 °C for the octadecyl compound, with a total of 80 carbons. Bolln et al. suggest that the upturn is a result of layering of the alkyl groups in these materials, as seen often for long alkyl chain appendages.[19] The crystal structure of the octa-*n*-octylsilsesquioxane, described by Bassindale et al., strongly supports this observation, as these molecules pack with four alkyl groups, forming layers to either side of the silsesquioxane core.[20]

At first glance, the upturn observed by Bolln et al. seems related to that observed here. However, our most pronounced upturn is for butyl groups with only hints of upturns for the other materials, especially those with the longest chain lengths, commensurate with the Bolln et al. compounds. We observe an upturn of 20 °C in the region where the total number of carbons on each OPS changes from (on average) 40 to 48. This is similar to the increments seen by Bolln et al., but the isobutyl/*n*-butyl mixture is very unlikely to layer. Consequently, we believe that the upturn in T_m and the exceptional increase in thermal stability results from interdigitation, which would limit the mobility of the alkyl branches with increasing degrees of substitution. We conclude this section by noting that the $T_{d5\%}$ of the hexyl compound with an average of 8 alkyl chains is >400 °C, but with 11 alkyl chains, $T_{d5\%}$ drops to 350 °C. It is reasonable to assume that interdigitation will eventually be obstructed as the number of alkyl chains per phenyl group increases, and thermal stabilities will decrease towards those of the longer-chain compounds.

Interdigitation is a well-known phenomenon in LC materials,[21–23] and often leads to changes in T_m and viscosity. However, the silsesquioxanes described here are very small spherical oligomers that have a single-crystal silica core, with only a limited relationship to linear LC polymers. Indeed, even the behavior here is unusual compared to the results described by Bolln et al.

Further support for our proposal comes from work by Esker et al., describing interdigitation in phenyl silsesquioxanes in Langmuir–Blodgett films.[24] These results provided the impetus to conduct molecular-dynamics simulations of alkyl$_x$OPS materials with varying chain lengths and degrees of substitution, in order to examine the chain–chain interactions in these systems. Figure 2 illustrates the local packing of the molecules. The modeling studies suggest that chain–chain interdigitation occurs in these systems, and appears to be more pronounced for alkyl$_x$OPS with shorter chains at higher degrees of substitution. Furthermore, they also suggest layering in the longest-chain materials. The modeling data in Figure 2

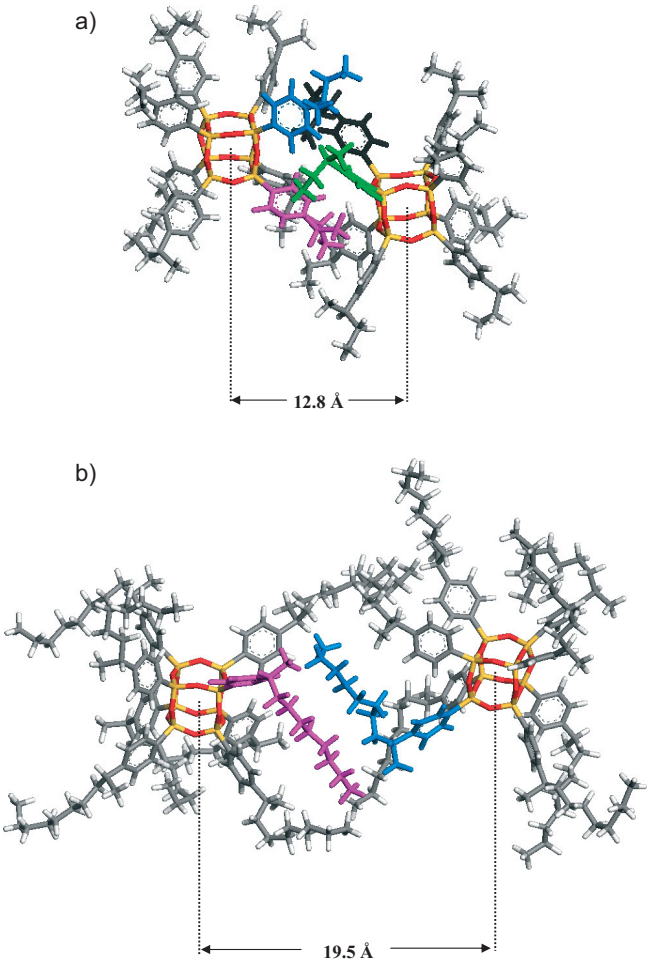

Figure 2. a,b) Molecular modeling of R$_x$OPS, where R = butyl (a) or R = decyl (b). In both cases, $x = 8$. Simulations were ran at 150 °C to capture liquid-state behavior.

suggest 12.8 and 19.5 Å core–core separations, versus 12.8 and 15 Å observed by XRD in the 10 h systems, supporting our conclusions. Additional support comes from recent theoretical studies on passivated metal-cluster assemblies (e.g., gold nanoparticles) stabilized with long-chain linear alkyl thiols, giving superlattices that are predicted to exhibit melting with interdigitation or layering of alkyl groups.[17] Such superlattice melting was recently observed.[18]

The current materials may be the smallest superlattice systems possible, or models thereof. Furthermore, the relatively high degree of ordering in solid alkyl$_x$OPS materials, coupled with the apparent ability to interdigitate, suggests that in the future it may be possible, with better control of the substitution patterns and structures of the alkyl groups, to make silsesquioxanes that mesh closely, as might be desired in a 3D gear structure. Alternately, the potential to interdigitate perhaps could be explored and expanded to develop nanoscale Velcro that forms strong mechanical locks near room temperature, but which on heating gives way to liquid structures that allow (nanoscale) components to be manipulated along surfaces.

Experimental

Materials: All reagent-grade chemicals were purchased from Aldrich or Fischer and used as-received, except for methylene chloride which was distilled from CaH_2 under N_2 prior to use. Octaphenylsilsesquioxane was purchased from Hybrid Plastics Co., or synthesized from phenyltrichlorosilane using Brown's method [10]. Phenyltrichlorosilane was donated by Clariant LSG, Gainesville, FL.

General Synthesis of Alkylated Phenylsilsesquioxanes: In a 100 mL Schlenk flask under N_2 flow were placed aluminum chloride (3.85 g, 28.9 mmol), 50 mL of CH_2Cl_2, and 50 mL of CS_2. Alkyl bromide (387 mmol) was then added via a syringe. The mixture was stirred at 0 °C for 15 min. OPS (5.0 g, 4.84 mmol, 38.7 mmol per phenyl group) was then added to the mixture with stirring. The solution was stirred at 0 °C for 5 h and then allowed to reach room temperature for an additional 19 h. Samples of 25 mL were drawn periodically. The samples were quenched by addition to 75 mL of water and 75 mL of hexane. The cloudy hexane layer was washed three times with water, and then filtered to remove insoluble fragmented silsesquioxane cages. The solvents were removed by evaporation in a rotary evaporator, and the orange liquids were distilled under vacuum at 150 °C to remove excess alkyl halide. The resulting liquids or solids were then dried in vacuo at 150 °C for 10 h. Yields ranged from 50–70 %.

Analytical Procedures: ^{1}H NMR and ^{13}C NMR were performed in $CDCl_3$ and recorded on a Varian INOVA 400 MHz spectrometer. ^{1}H NMR spectra were collected at 400.0 MHz by using a spectral width of 6000 Hz, a relaxation delay of 3.5 s, 30 k data points, a pulse width of 38°, and $CHCl_3$ (7.27 ppm) as an internal reference. ^{13}C NMR spectra were collected at 100.6 MHz by using a spectral width of 25 000 Hz, a relaxation delay of 1.5 s, 75 k data points, a pulse width of 40°, and $CDCl_3$ (77.23 ppm) as an internal reference.

Thermal stabilities of the materials were tested under air using a TA Instruments 2960 simultaneous DTA-TGA instrument (TA Instruments, Inc., New Castle, DE). Samples (10–20 mg) were heated under vacuum at 60 °C for a minimum of 6 h prior to analysis, and heated to 120 °C (10 min) inside the TGA before analysis to remove any adsorbed water.

Diffuse-reflectance IR spectrometry (DRIFTS) was performed using a Mattson Galaxy 3000 spectrometer (Mattson Instruments, Inc.). Optical grade potassium bromide (International Crystal Laboratories, Garfield, NJ) was used as the background material. Samples (1–3 mg) were ground with KBr (500 mg) in an alumina mortar and pestle, packed into a sample holder, and smoothed using a glass microscope slide. The spectra were recorded under dry N_2 purge, and consisted of 128 scans at a resolution of ca. 4 cm^{-1}.

All GPC analyses were performed on a Waters 440 system equipped with Waters styragel columns (7.8 × 300, HT2, 3, 4) with RI detection, using an Optilab DSP interferometric refractometer and tetrahydrofuran as solvent. The system was calibrated using polystyrene standards and toluene as reference.

Melting points were determined on a Laboratory Devices Mel-Temp apparatus. Samples were placed in open capillary tubes and heated at a rate of ca. 1 °C min^{-1}. Melting-point ranges were determined visually.

DSC traces were recorded on a 2910 Differential Scanning Calorimeter (TA Instruments, Inc., New Castle, DE) under N_2. The calorimeter was calibrated using indium as a reference. Samples (10–15 mg) was placed in a pan and heated at 3 °C min^{-1} to a temperature at least 50 °C above the melting point.

Viscosities of all systems were measured using a parallel plate Rheometric RDS II E system at a shear rate of 10 s^{-1}, with a gap of 1 mm.

Molecular Modeling Methods: Molecular modeling was carried out using the Discover module of the Materials Studio modeling and simulation suite (Accelrys, Inc.). Molecular mechanics and molecular dynamics (MD) simulations were performed in vacuum using the COMPASS force field. $Alkyl_x$OPS monomers were initially energy-minimized using a combination of the steepest-descent and conjugate-gradient methods for a total of 1000 iterations to relax intramolecular structural quantities (bond lengths, bond angles, and torsion angles) to their equilibrium values and to eliminate artifacts from the drawing process. These monomers were duplicated and MD simulations were conducted in a canonical ensemble at 1000 K for 500 ps to relax the initial configurations. The MD simulations were then continued at the target temperature of 423 K (150 °C) in an isothermal–isobaric ensemble using periodic boundary conditions and the Berendsen barostatting and thermostatting methods. These simulations were performed with a 1 fs time step for a total of 2 ns. Both the potential energy and simulation box length profiles were monitored during the simulations to ensure that each system was in equilibrium.

Received: July 11, 2006
Revised: October 6, 2006
Published online: December 12, 2006

[1] a) M. G. Voronkov, V. I. Lavrent'yev, *Top. Curr. Chem.* **1982**, *102*, 199. b) R. H. Baney, M. Itoh, A. Sakakibara, T. Suzuki, *Chem. Rev.* **1995**, *95*, 1409. c) A. Provatas, J. G. Matisons, *Trends Polym. Sci.* **1997**, *5*, 327. d) J. Lichtenhan, in *Polymeric Materials Encyclopedia*, Vol. 10 (Ed: J. C. Salmone), CRC, New York **1996**, p. 7768. e) R. M. Laine, *J. Mater. Chem.* **2005**, *15*, 3725.

[2] a) *Organic/Inorganic Hybrid Materials* (Eds: R. M. Laine, C. Sanchez, C. J. Brinker, E. Giannelis), MRS Symposium Series, Vol. 628, Materials Research Society, Pittsburgh, PA **2000**. b) *Organic/Inorganic Hybrid Materials* (Eds: C. Sanchez, R. M. Laine, S. Yang, C. J. Brinker), MRS Symposium Series, Vol. 726, Materials Research Society, Pittsburgh, PA **2002**.

[3] a) J. W. Gilman, D. S. Schlitzere, J. D. Lichtenhan, *J. Appl. Polym. Sci.* **1996**, *60*, 591. b) R. I. Gonzalez, S. H. Phillips, G. B. Hoflund, *J. Spacecr. Rockets* **2000**, *37*, 463. c) A. L. Brunsvold, T. K. Minton, I. Gouzman, E. Grossman, R. I. Gonzalez, *High Perform. Polym.* **2004**, *16*, 303.

[4] a) A. J. Waddon, E. B. Coughlin, *Chem. Mater.* **2003**, *15*, 4555. b) S. A. Gromilov, T. V. Basova, D. Yu, Emel'yanov, A. V. Kuzmin, S. A. Prokhorova, *J. Struct. Chem.* **2004**, *45*, 471.

[5] a) F. J. Feher, D. A. Newman, J. F. Walzer, *J. Am. Chem. Soc.* **1989**, *111*, 1741. b) F. J. Feher, T. A. Budzichowski, R. L. Blanski, K. J. Weller, J. W. Ziller, *Organometallics* **1991**, *10*, 2526. c) T. Maschmeyer, M. C. Klunduk, C. M. Martin, D. S. Shephard, J. M. Thomas, B. F. G. Johnson, *Chem. Commun.* **1997**, 1847. d) F. J. Feher, R. L. Blanski, *J. Am. Chem. Soc.* **1992**, *114*, 5886. e) F. J. Feher, D. Soulivong, A. G. Eklud, K. D. Wyndham, *Chem. Commun.* **1997**, 1185. f) J. R. Severn, R. Duchateau, R. A. van Santen, D. D. Ellis, A. L. Spek, *Organometallics* **2002**, *21*, 4.

[6] a) E. S. Baker, J. Gidden, S. E. Anderson, T. S. Haddad, M. T. Bowers, *Nano Lett.* **2004**, *4*, 779. b) M. H. Lamm, T. Chen, S. C. Glotzer, *Nano Lett.* **2003**, *3*, 989.

[7] N. Maxim, P. C. M. M. Magusin, P. J. Kooyman, J. H. M. C. van Wolput, R. A. van Santen, H. C. L. Abbenhuis, *J. Phys. Chem. B* **2002**, *106*, 2203.

[8] C. Bonhomme, D. Toledano, J. Maquet, J. Livage, L. Bonhomme-Coury, *J. Chem. Soc., Dalton Trans.* **1997**, 1617.

[9] A. R. Bassindale, M. Pourny, P. G. Taylor, M. B. Hursthouse, M. E. Light, *Angew. Chem. Int. Ed.* **2003**, *42*, 3488.

[10] J. F. Brown, Jr., L. H. Vogt, P. I. Prescott, *J. Am. Chem. Soc.* **1964**, *86*, 1120.

[11] K. Olsson, C. Grönwall, *Ark. Kemi* **1961**, *17*, 529.

[12] a) R. Tamaki, Y. Tanaka, M. Z. Asuncion, J. Choi, R. M. Laine, *J. Am. Chem. Soc.* **2001**, *123*, 12 416. b) J. Choi, J. Harcup, A. F. Yee, Q. Zhu, R. M. Laine, *J. Am. Chem. Soc.* **2001**, *123*, 11 420.

[13] a) C. Brick, R. Tamaki, S.-G. Kim, M. Asuncion, M. Roll, T. Nemoto, Y. Chujo, R. M. Laine, *Macromolecules* **2005**, *38*, 4655. b) C. M. Brick, Y. Ouchi, Y. Chujo, R. M. Laine, *Macromolecules* **2005**, *38*, 4661.

[14] *Friedel-Crafts Chemistry* (Ed: G. A. Olah), Wiley, New York **1973**.

[15] T. H. Chan, I. Fleming, *Synthesis* **1979**, 761.

[16] R. Blanski, J. Leland, B. Viers, S. H. Phillips, *Internat. SAMPE Symp. Exhib.* **2002**, *47*, 1503.
[17] U. Landman, W. D. Luedtke, *Faraday Discuss.* **2004**, *125*, 1–22.
[18] P. Sandhyarani, J. Chakrabarti, M. Yousuf, H. K. Sahu, *Phys. Rev. B: Condens. Matter Mater. Phys.* **2000**, *62*, 739.
[19] C. Bolln, A. Tsuchida, H. Frey, R. Mulhaupt, *Chem. Mater.* **1997**, *9*, 1475.
[20] A. R. Bassindale, H. Chen, Z. Liu, I. A. MacKinnon, D. J. Parker, P. G. Taylor, Y. Yang, M. E. Light, P. N. Norton, M. B. Hursthouse, *J. Organomet. Chem.* **2004**, *689*, 3287.
[21] S. J. Holder, J. A. A. W. Elemans, J. J. J. M. Donners, M. J. Boerakker, R. D. Gelder, J. Barbera, A. E. Rowan, R. J. M. Nolte, *J. Org. Chem.* **2001**, *66*, 391.
[22] R. A. Kloster, M. D. Carducci, E. A. Mash, *Org. Lett.* **2003**, *5*, 3683.
[23] C. W. Struijk, A. B. Sieval, J. E. J. Dakhorst, M. van Dijk, P. Kimkes, R. B. M. Koehorst, H. Donker, T. J. Schaafsma, S. J. Picken, A. M. van de Craats, J. M. Warman, H. Zuilhof, E. J. R. Sudhölter, *J. Am. Chem. Soc.* **2000**, *122*, 11 057.
[24] J. Deng, J. T. Polidan, J. R. Hottle, C. E. Farmer-Creely, B. D. Viers, A. R. Esker, *J. Am. Chem. Soc.* **2002**, *124*, 15 194.

